The Pennsylvania State University
Wind Energy Club

Technical Design Report

Submitted to
2021 Collegiate Wind Competition
NREL Competition Operations Manager Elise DeGeorge

Aerodynamics Team

Joshua Forrest	Lead
Joshua Bannon	Member
Allison Karp	Member
Akhilesh Mulgund	Member
Jeremy O'Connor	Member
Joseph Snider	Member
Colin Welch	Member

Circuits and Controls Team

Jackie Cheng	Lead
Satyam Patel	Lead
Mohammed Aal Abdulla	Member
James Leandri	Member

Generator Team

Eric Sarbacker	Lead
Eric Folmar	Member
Tara Presnall	Member
Zoe Shu	Member

Strategic Advisors

Dr. Mark Miller
Dr. Susan Stewart
Dr. Yan Li
Mr. Richard Auhl
Jason Cornelius
Costa Kandias
Sean Wang

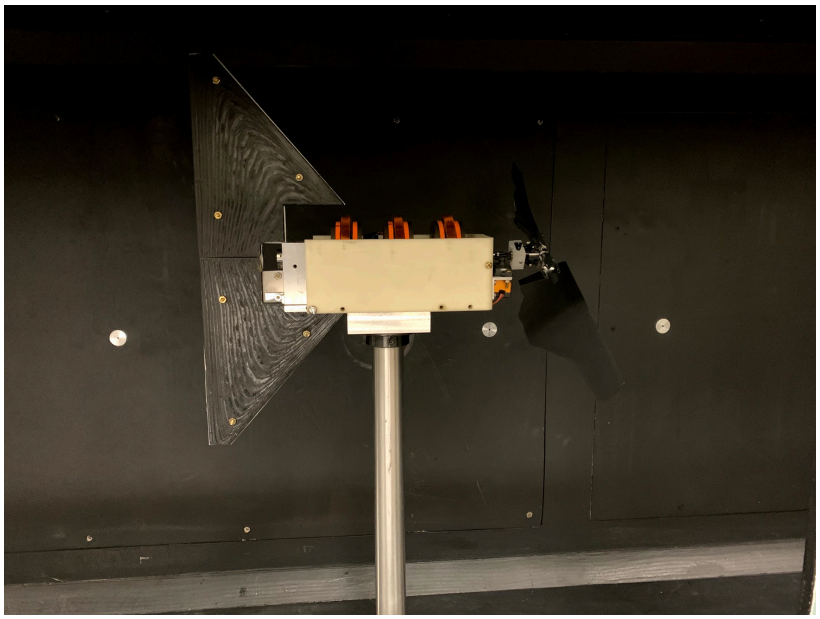

Table of Contents

1 Executive Summary

In this document, the Pennsylvania State University Wind Energy Club describes the research, design, construction, and analysis of a wind turbine during the Covid-19 pandemic. The team divided the turbine system into three primary categories: aerodynamics, generator, and circuits and control. The team overcame many challenges derived from the pandemicand also had to make many compromises. In particular, the inability to access any laboratory spaces until the middle of March hindered progress in the assembly and experimentation for the turbine. However, the team made significant strides in the system's design.

The wind turbine system features a newly-designed two-bladed rotor with the potential for increased torque at startup and higher power coefficients across Region II operation. The turbine's pitching servo has transitioned from a radial to linear servo to more precisely and accurately control the pitching of the blades. The generator used is an axial-flux three-stage generator that minimizes the torque required. The control circuit for the turbine uses an arduino to control the pitching servo and also varies the circuit load to maximize and control the power produced by the turbine as well as meet the competition requirements for voltage.

Overall, the 2021 competition turbine builds upon the team's previous successes with turbine design and features an improved rotor, pitching system, and control circuit.

2 Technical Design

The Turbine was split into 3 subsystems/sub-teams: The Aerodynamics team was responsible for the design of the blades, the Circuits and Control team was responsible for controlling the pitch and electrical systems, and the Generator team was responsible for the generator's physical design and optimization. Each sub-team met on their own once per week in addition to meeting with the entire team to discuss their work and progress on their subsystem of the turbine.

2.1 Rotor System Design

This year, the Aero sub-team decided to switch to a 2-bladed rotor design. Much of the fall semester was focused on determining whether this was the right choice, and additionally was tasked with finding a suitable airfoil for the blades. This process was done first using XFOIL to determine which airfoil would have the best lift-to-drag characteristics and secondly in XTURB (a Blade Element Momentum performance code developed at Penn State) to narrow down the shape of our blades [2, 3]. Once we had the shape determined, we began to create a SolidWorks model of the blade by outlining the shape of the blade along the span, pasting the airfoil coordinates along 52 planes of the blade, and rotating each airfoil to the ideal twist according to our simulations in XTURB. Once the model was complete around the middle of the spring semester, the blades were ready to be 3D printed. The initial prints of our blades were flimsy and tessellated near the thin trailing edge, and they

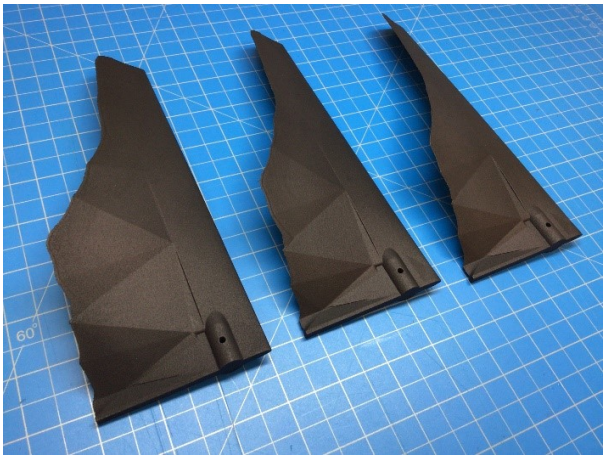

Figure 1: The Nylon 12 material blades experienced high tip deflections and were prone to flutter

tended to flutter when tested in the wind tunnel. As such, another company was chosen for printing a second batch using a different material, and these new blades were stronger and much more accurate when compared with the CAD model (Figure 2).

2.1.1 Rotor Design

Wind turbine rotor design depends heavily on the scale of the rotor which drives the limiting design factors. The scale of utility wind turbines is so large that the primary limiting design factors are the maximum allowable tip speed and blade structural design. The industry has converged primarily on 3-bladed rotors because they effectively produce power while meeting requirements for noise and relatively affordable construction. However, the CWC rotors are only 45 cm in diameter, which makes the aerodynamics of the rotor the limiting factor rather than the rotor structure or tip speeds. More specifically, a large contributor to the rotor's deviation from a rotor's optimal performance is the low blade chord Reynolds numbers. At lower Reynolds numbers, airfoils have significantly higher drag coefficients. For the MA 409 airfoil used in this turbine, the drag coefficient at the airfoil's most efficient point (or maximum glide ratio) is 0.0221 at 50,000 Reynolds number and 0.0134 at 110,000 Reynolds number, obtained from XFOIL [2]. That is a 39% decrease in relative drag due to the increase in Reynolds number. Because the drag decreases with increasing Reynolds number, the glide ratio, or the ratio of lift to drag, also increases with Reynolds number. The rotor's aerodynamic performance increases with an increase in the glide ratio, so the rotor design emphasized maximizing the glide ratio of the blades.

Figure 2: Accura60 material blades are stiffer than the Nylon 12 blades.

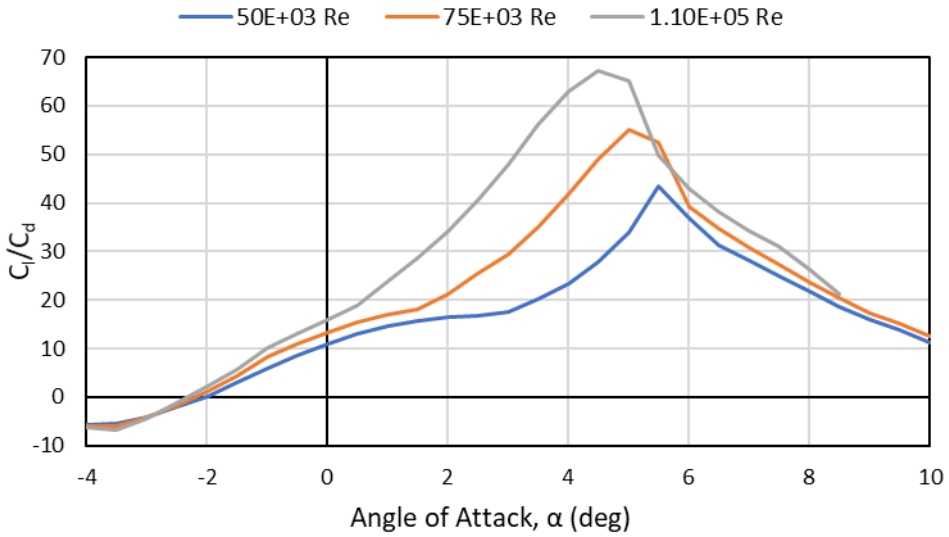

Figure 3: MA 409 airfoil "Glide Ratio" for expected Reynolds numbers

Increasing Reynolds number can be achieved in four different ways: an increase in the fluid density, a decrease in the fluid viscosity, an increase in the fluid flow speed, or an increase in the length scale of the aerodynamic body. In the competition, the only parameter that can be adjusted is the length scale of the aerodynamic body: the blade chord length. However, increasing the blade chord length changes the rotor solidity and reduces the maximum power coefficient tip speed ratio. From Aerodynamics of Wind Turbines, the best design tip speed ratio depends upon the average expected airfoil glide ratios along the blade in the design case [4]. For the competition, the highest-scoring category in the power curve task is 8 m/s, for which the rotor is expected to have chord Reynolds numbers of approximately 40,000 to 70,000 along the blade for the club's 3-bladed rotor from 2020. At these Reynolds numbers, most airfoils achieve glide ratios of 25 to 40 according to XFOIL. This corresponds to a design tip speed ratio of approximately 3.5, which is the 2020 rotor design point ([4], figure 3.14). If the average glide ratio is increased by increasing the Reynolds number, the rotor will have a higher power coefficient across all tip speed ratios. However, simply increasing the chord of the blades will increase the solidity and decrease the maximum power coefficient tip speed ratio and the rotor will under perform. Instead, reducing the number of blades to two and increasing the chord allows for the solidity to be slightly decreased while increasing Reynolds number. This allows for the tip speed ratio to be 4, which was determined to be the design case after evaluating available airfoils at the expected Reynolds numbers, discussed later on.

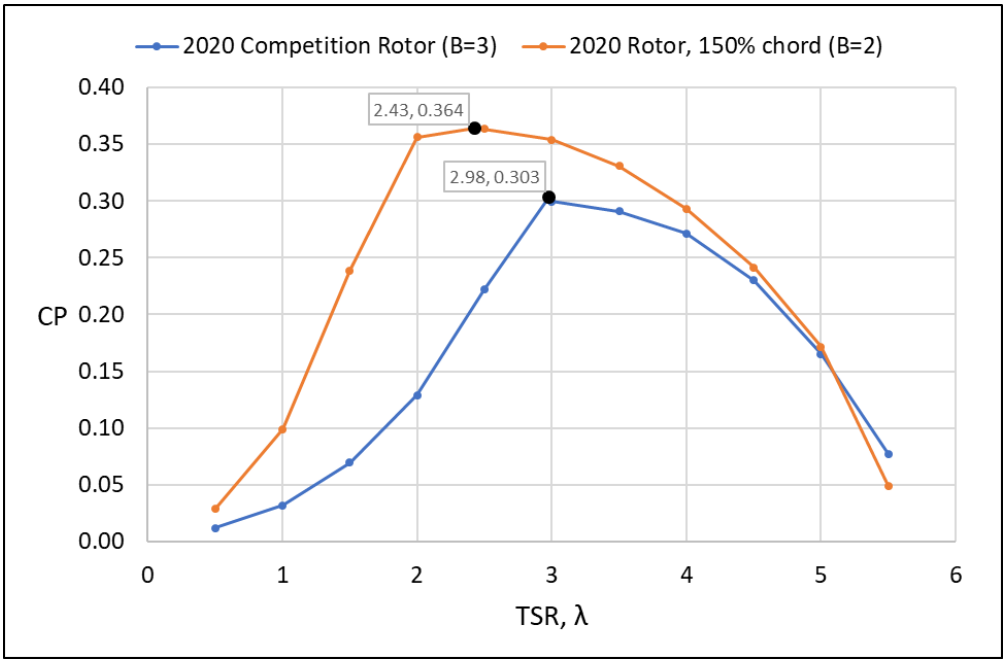

Figure 4: Power curves for the PSU 2020 3-blade competition rotor and 2-blade change

Changing to a two-bladed rotor with a longer chord length increases the Reynolds numbers to improve rotor performance but also increases the tip losses which decrease rotor performance. To investigate the tradeoffs between the two effects, the 2020 competition rotor design was analyzed in XTURB in the original 3-bladed configuration and a comparison 2-bladed case with chord of the blades increased by 50% to match the solidity. The two designs were compared at a fixed pitch which was optimized for the design tip speed ratio of the 3-bladed rotor. As shown in Figure 4, the maximum power coefficient increased by 20.1% from 0.303 to 0.364. Importantly, the power coefficient was increased across all tip speed ratios, notably at low tip speed ratios. This is due to the increased Reynolds number delaying the onset of stall, which occurs for a fixed-pitch turbine at low tip speed ratios. This indicates the potential for more torque at low wind speeds

with the two-bladed rotor compared to the three-bladed rotor.

The two-bladed rotor was designed using a procedure based on the ideal Blade number, tip speed ratio, lift coefficient, and chord relation described by in [4]. Given a defined blade number, design tip speed ratio, and design lift coefficient distribution, the chord distribution of the blades can be determined.

$$\mathrm{B}\lambda c_l * \mathrm{c}(r/R) = \left(\frac{4}{3}\right)^2 \pi \frac{1}{\lambda_r} \tag{1}$$

Once an airfoil is selected, the pitch distribution can also be obtained by determining the design angle of attack required to achieve the design lift coefficient. The design lift coefficient is determined by choosing the optimal glide ratio lift coefficient for the chosen airfoil.

To select the optimal airfoil, a number of different airfoils from the Selig Airfoil Database were analyzed using XFOIL. The glide ratios vs angles of attack were plotted for the lower Reynold's number of 50,000. It was found that the MA 409 airfoil had the highest peak glide ratio compared to other airfoils [5]. Further optimization to the design could involve searching for airfoils that have a more rounded peak at the higher glide ratios rather than the sharp peak found in the MA 409.

Once the MA409 airfoil was selected, the blade was designed using Equation 1 as a first-pass. The design was altered to reduce the chord towards the inboard sections to a more reasonable chord length and rounding the tip off to reduce tip losses. The resulting design was analyzed in XTURB to determine the expected performance (Figure 5).

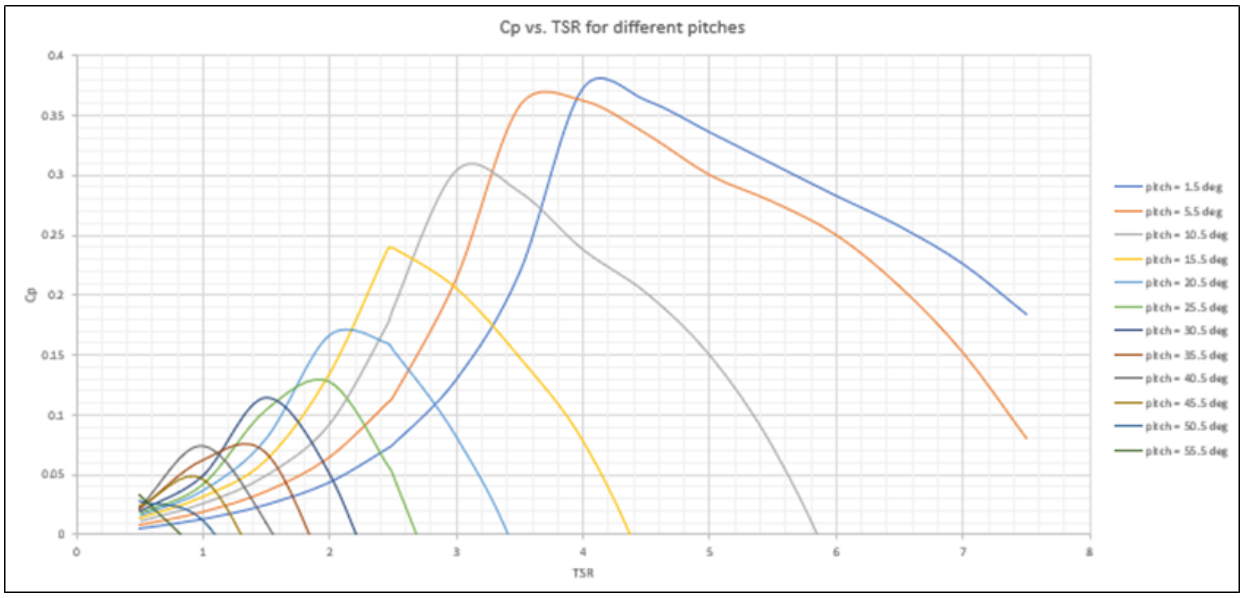

Figure 5: Power curves for the PSU 2021 two-bladed competition rotor with varying collective pitches.

The power coefficient curve was determined for a variety of collective pitches. The results show that the optimum power coefficient of 0.38 is achieved for a collective pitch of 1.5 degrees for a tip speed ratio of 4.1. This is a significant improvement of 25.4% in peak power coefficient compared to the 2020 rotor design. Increasing the collective pitch of the blades increases the rotor's power coefficient at lower tip speed ratios. This clearly indicates the control procedure for the turbine when in operation in regions 2 and 3. The startup pitch is likely to be much higher, so pitching the blades out of the wind from the startup pitch will increase the rotor speed to the optimum tip speed ratio. However, experimentation to determine the exact pitches is required to verify the results from XTURB. Performing these experiments is the goal of the club for the 2022 Competition due to limited access to on-campus activities for the 2021 Competition.

2.1.2 Rotor Structural Testing

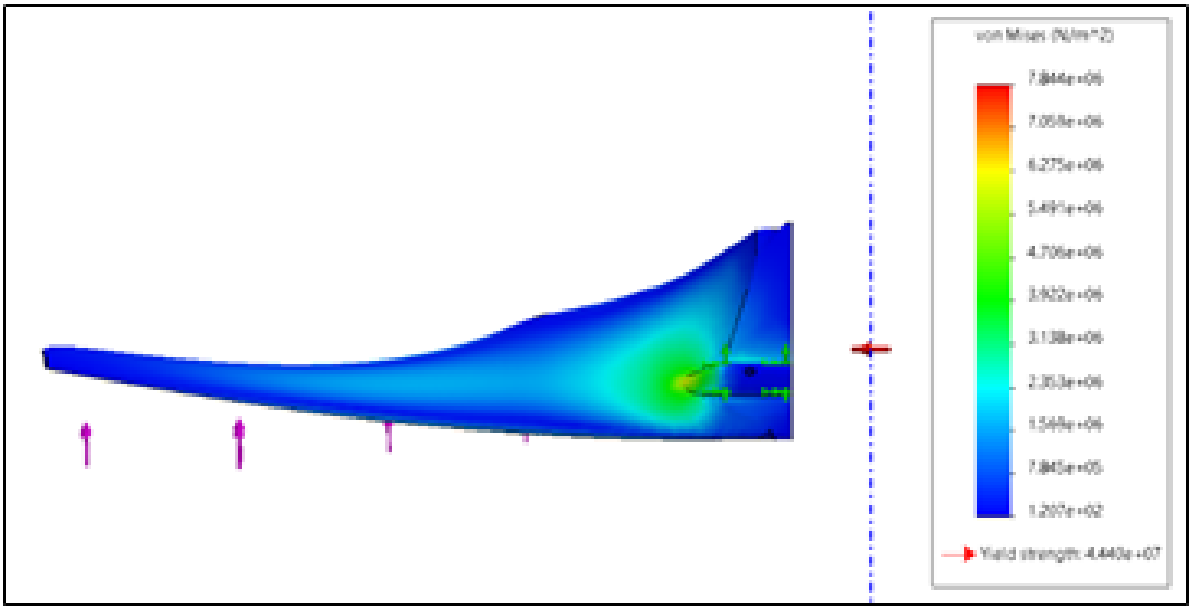

Figure 6: Visualization of blade stresses for the highest load case, 23 m/s freestream and 1867 RPM. There is a stress concentration at the gripped location but the stress is below the yield stress by a factor of 5.66.

From our SolidWorks testing of our blade design, it was clear that the most stress would be at the end of the circular piece that connects the blade to the hub. The loads applied were informed by XTURB results. XTURB gives a distribution of lift coefficient, from which the spanwise lift distribution was determined. A fifth-order polynomial was curve-fit to the spanwise distribution of lift with an R^2 value of 0.985. The loads were applied normal to a strip centered at the blade's quarter-chord, which was estimated to be the approximate aerodynamic center. The total scaling of the loads applied was changed to match the total thrust from aerodynamic forces, in this case 45 N for each blade for the 23 m/s case. Then, the centripetal load from rotating 1867 RPM was applied and the resultant stresses analyzed for stress concentrations and factors of safety. Our strength results, with a Nylon 12 material imported in, demonstrated a factor of safety of 5.66 (Figure 6) for the max load of 45 N.

Figure 7: Blade strength testing to verify the factor of safety. The load applied was resolved to the spanwise location of the resolved lift distribution at the quarter chord. The Nylon 12 blades had high strain but did not yield.

To confirm the SolidWorks simulations, the blades were tested physically in person. The blades used in this experiment contain the same airfoil used in the model and have the same shape, but they are not the final blades used for our turbine. Due to limited time and restrictions on in-person work due to the pandemic, only a single set of blades were available for testing and these had a manufacturing defect on the pressure side of the blade. However, it was expected that this discrep-

ancy would not significantly affect the performance of the test and would still produce useful validation data for our final product. The setup involved fixing the blade at the hub location with a clamp. This was done in order to straighten the other end of the blade to easily add weights at the resultant force location to accurately represent the aerodynamic blade loads. From here, weights were added one at a time until the point of failure. However, the failure occurred due to the clamping system, not by breakage of the blade. Until this point, the blade was able to withstand over 62 N which guarantees a factor of safety of at least 1.77. However, the competition rules state that the maximum testing done in competition will be 13 m/s, not 23 m/s. This means that the maximum aerodynamic loading will be 11.2 N in the actual competition testing. Compared to this loading case, the factor of safety is at least 5.53. It is noted in the image of the test that the blade was bending significantly which is undesirable for a wind turbine. Because of this we decided to reconsider our material to Accura 60, which is significantly stiffer. However, the team was unable to test the new Accura 60 blades and will look to analyze their structural factor of safety for the 2022 competition.

2.1.3 Hub Strength Testing

The hub testing was completed in a similar way to past competition rotors. A block with a rod on one end is clamped to an I-beam attached to the wall. This rod took the place of the generator driveshaft and locates the hub piece. A sacrificial bolt was used where the blade would normally be clamped in case of damage it could be easily removed. Once the bolt was in place with the hub on the rod, a chain hoist was used to apply an upward force on the hub assembly, with the resulting force being read out by a dial gauge between the hoist and hub. From the SolidWorks model, it was predicted that the hub needed to withstand approximately 110 N on each side to fully support the blades at their maximum speed. The hub was tested up to 890 N with only minor damage to the screw. This creates a factor of safety of at least 8.09 which means our strength test proved to be very successful and the blades will be held without damage.

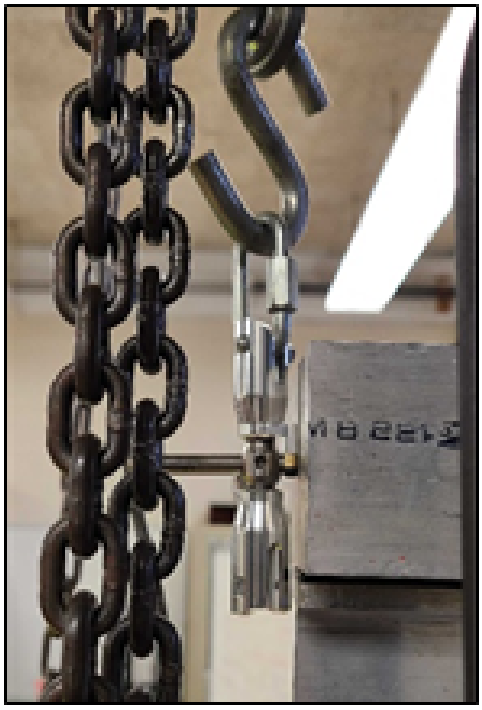

Figure 8: Testing the strength of the hub for radially applied tension force equal to the blades spinning at 1867 RPM.

2.1.4 Blade Collective Pitch System

The rotor hub was changed to support the shift to the two-bladed design. A re-purposed RC helicopter tail rotor (Align 700) was used [1]. This device, when paired with the two linear servos, will be able to pitch the blades at a variety of different angles for the cut in wind speed, power curve performance, and safety tasks. In the past, radial servos have been used, with preliminary investigations also exploring using linear servos. It was found that two linear servos in parallel would draw similar power to the single radial servo. The two linear servos will be located on either side of the nacelle. This will ensure that no bending moment is created on the shaft of the nacelle when setting the blade pitch, a problem that was faced in previous years' designs. These designs were made remotely using CAD software, with measurements of the different parts taken by team members who were in-person.

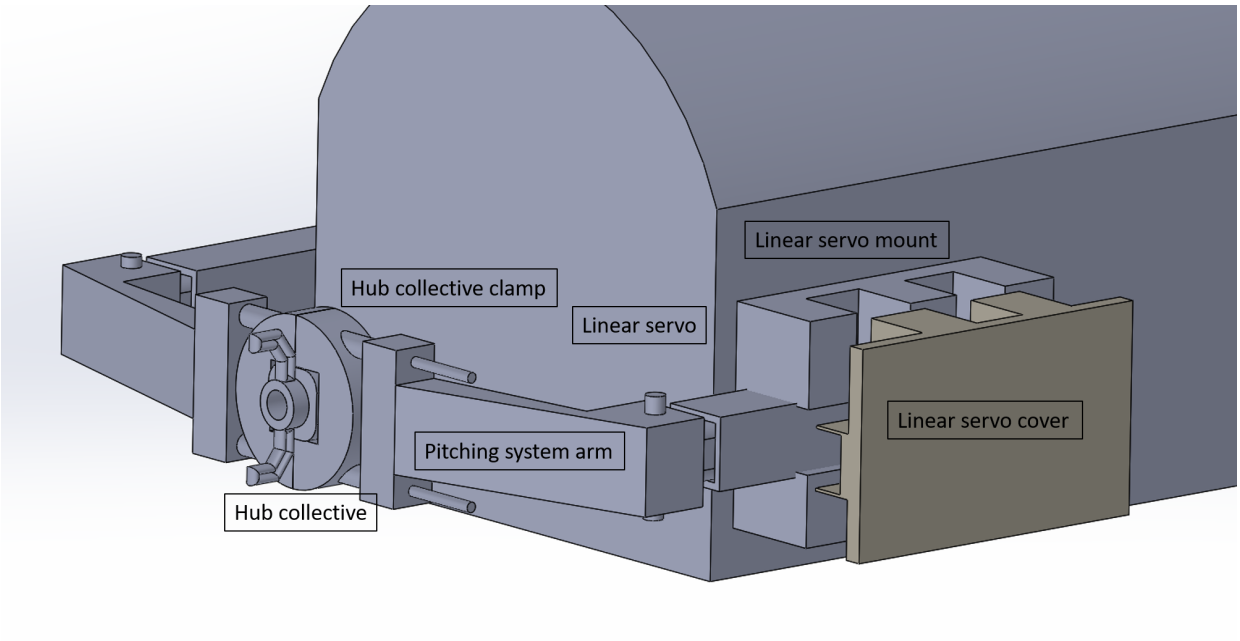

Figure 9: Linear servo pitching system with dual linear servos controlled simultaneously by the arduino.

2.1.5 Yaw Control System

Our yaw system is entirely passive and unpowered. It relies on a tailfin, composed of steel and a 3D printed NACA 009 airfoil. This design is more than capable of moving our turbine into the direction of the freestream air, and it does so without needing any active control or power. Two halves of the airfoil sandwich the metal plate, which is attached to the rear of our turbine nacelle via screws. An in-depth analysis of how quickly the tailfin can yaw the turbine depending on the velocity of the oncoming air has not been performed as of the writing of this report. However, based on how the turbine performs in the wind tunnel, it appears return the nacelle to the freestream direction within 1-2 seconds.

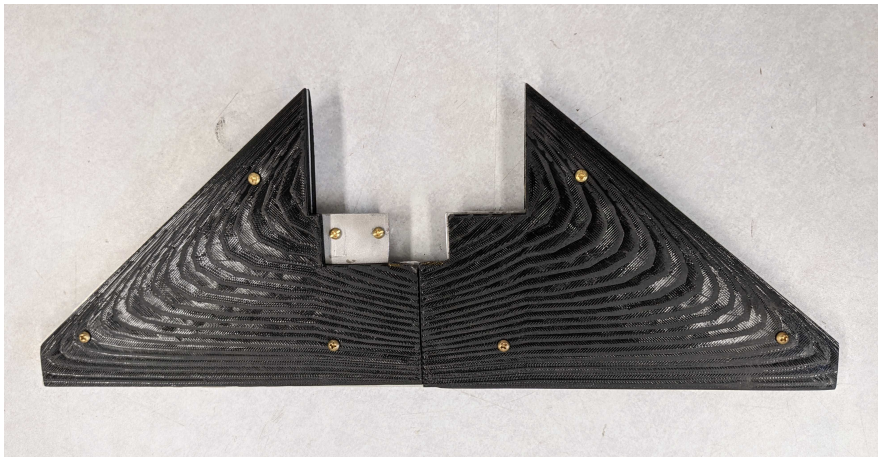

Figure 10: The turbine tailfin, which is a flat metal plate with 3D printed NACA 009 covers.

2.2 Generator Design

For the generator sub-team, much of the year was spent with the generator inaccessible, so most of the efforts were focused on improving the generator design code that is used to predict performance. The generator code was redesigned so that new members of the team would understand how to use it. This came in the form of adding additional graphs as well as explanations of what the code uses for its calculations. With all these additions to the code, we hope that new members will be able to use the code, understand what it is outputting, and be able to more systematically change the variables to see how it would affect generator performance.

Prediction of Voltage, Current, Electrical Power

	Voltage			Current			Power			
RPM	1	2	3	1	2	3	1	2	3	
200	1.05	2.09	3.14	0.180	0.180	0.180	0.19	0.38	0.57	
400	2.09	4.18	6.27	0.360	0.360	0.360	0.75	1.51	2.26	
600	3.14	6.27	9.41	0.540	0.540	0.540	1.70	3.39	5.09	
800	4.18	8.36	12.55	0.721	0.721	0.721	3.01	6.03	9.04	
1000	5.23	10.45	15.68	0.901	0.901	0.901	4.71	9.42	14.13	
1200	6.27	12.55	18.82	1.081	1.081	1.081	6.78	13.56	20.34	
1400	7.32	14.64	21.95	1.261	1.261	1.261	9.23	18.46	27.69	
1600	8.36	16.73	25.09	1.441	1.441	1.441	12.05	24.11	36.16	
1800	9.41	18.82	28.23	1.621	1.621	1.621	15.26	30.51	45.77	
1900	9.93	19.86	29.80	1.712	1.712	1.712	17.00	34.00	50.99	
2000	10.45	20.91	31.36	1.802	1.802	1.802	18.83	37.67	56.50	
2200	11.50	23.00	34.50	1.982	1.982	1.982	22.79	45.58	68.37	Target
2400	12.55	25.09	37.64	2.162	2.162	2.162	27.12	54.24	81.37	
2600	13.59	27.18	40.77	2.342	2.342	2.342	31.83	63.66	95.49	
2800	14.64	29.27	43.91	2.522	2.522	2.522	36.92	73.83	110.75	
3000	15.68	31.36	47.05	2.702	2.702	2.702	42.38	84.76	127.13	
3200	16.73	33.45	50.18	2.883	2.883	2.883	48.22	96.43	144.65	
3400	17.77	35.55	53.32	3.063	3.063	3.063	54.43	108.86	163.30	
3600	18.82	37.64	56.45	3.243	3.243	3.243	61.02	122.05	183.07	
3800	19.86	39.73	59.59	3.423	3.423	3.423	67.99	135.99	203.98	
4000	20.91	41.82	62.73	3.603	3.603	3.603	75.34	150.68	226.02	

$$V = \frac{2\,\pi\,q\,k\,\emptyset}{120} * \frac{N}{\sqrt{2}} * Stators$$

$$I = \frac{V}{2 * R} * Stators$$

$$P = I * R * Stators$$

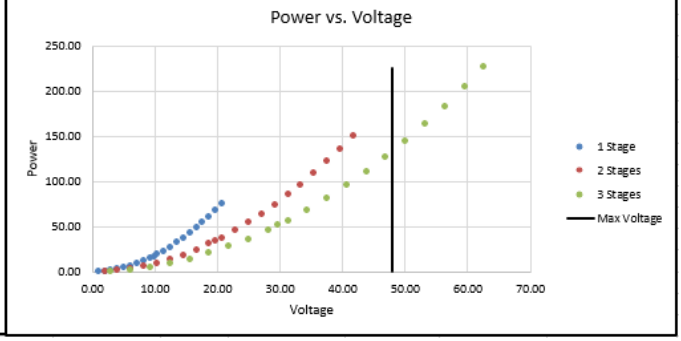

Figure 11: Updated V, I, P section of the generator code includes range of values along various RPM values, highlighting the target value for the turbine at max RPM. Now also includes how the values were calculated as well as important graphs highlighting range of power in compliance with competition safety.

The prediction of voltage, current, and electrical power is just one small portion of the generator code. The updated version gives a clearer picture of the design process and accomplished what we aimed for in making the design good looking as well as more accessible.

Although the generator code is helpful in the prediction of how the generator will perform, all calculations should be backed up by rigorous testing. Testing is not only important to validate the predictions of the generator code, but also ensure the generator can withstand the conditions it is required to undertake. If any components of the generator are not working properly, then it is much easier to fix the problem outside of the wind tunnel, for this reason we did most testing on a dynamometer test bench.

To improve on generator testing this year, upgrades were made to our dynamometer test stand to

allow for testing and changes to be made to the generator on the fly. Compared with previous years, the generator is placed upright on the test stand. Additionally, this new design is more secure than in previous years. By using bolts and machined aluminum rather than metal straps, there are less vibrations and less unwanted torques on the generator and dynamometer.

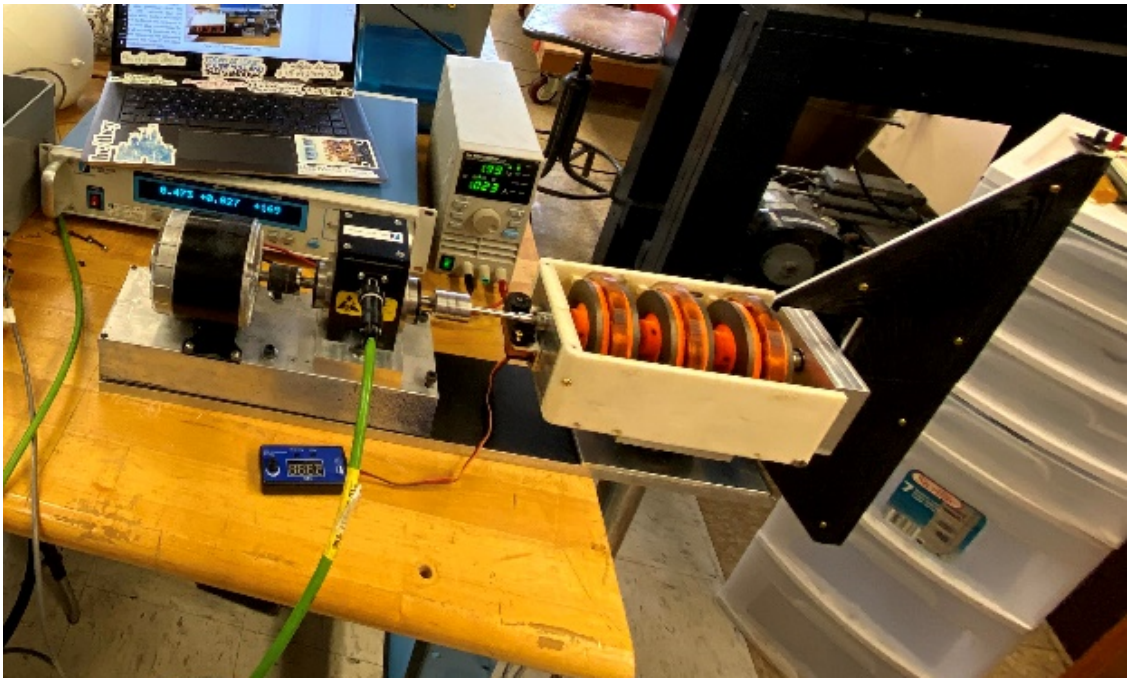

Figure 12: Generator dynamometer testing set up.

The data collected from the dynamometer testing was limited due to lab access being restricted, but the test did validate the generator code and proved that the generator performs as required, even outside the range that is necessary for competition. The data collected on variable resistance will be helpful in optimizing load resistance and power output for possible automation in the future.

Since the generator was mostly unavailable, the parts of the generator were reused from last year. The turbine structure was made from aluminum and steel parts and constructed using traditional machining techniques. This includes the tower baseplate, nacelle structure, shaft, and servo connector. The housing, and generator rotors were best constructed out of ABS plastic with fused deposition modeling 3D printing, which is very accurate but does not produce as strong a final product as traditional machining does with metals. For this reason, the plastic parts are designed not to be structural and take minimal loads. During testing, imperfections were found in the nacelle that hinder the performance and accessibility of the stators. Plans were made to improve the housing to relieve these issues, but they were never realized as getting initial testing done was deemed more important.

2.3 Turbine Nacelle

The turbine structure was constructed using traditional machining techniques, with high-strength aluminum and steel parts with relatively simple geometries. The tower baseplate, nacelle structure, shaft, and servo connector were made using this technique. The housing, and generator rotors however, have very complex geometries that are best constructed out of ABS plastic with fused deposition modeling 3D printing. This technique is very accurate but does not produce as strong a final product as traditional machining does with metals. For this reason, the plastic parts are designed not to be structural and take minimal loads.

2.4 Circuits and Control Design

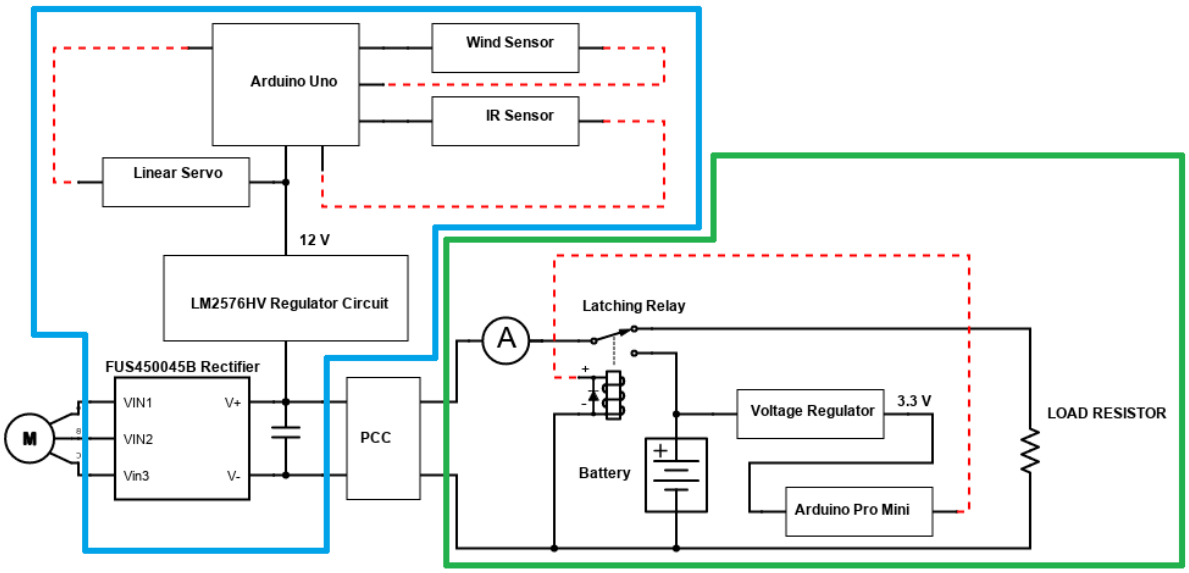

Figure 13: Complete Electrical Diagram- the blue outline encompasses the control circuit and the green outline encompasses the load circuit.

2.4.1 Voltage Rectification

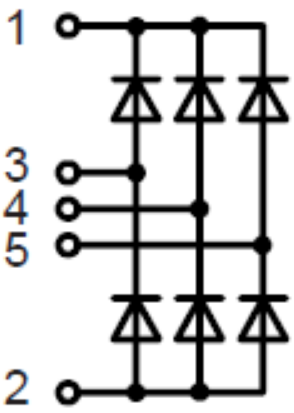

Figure 14: Diagram of FUS45-0045B

The generator produces an AC signal with nine total phases of output voltage. A total of three Schottky Three Phase Bridge Rectifiers inside a FUS45-0045B IC are used to convert the 9 phased AC signal to a single DC signal. A single 3 phase rectification circuit is shown in Figure 14. The maximum input of the rectifier is 45VRRM outputting up to 63V DC. This is well within the range of operation because the voltage across the PCC cannot exceed 48V. This DC signal can now be used to feed the computers and sensors within the turbine, and most importantly, power the turbine load. The complete electrical diagram of the turbine control and load circuit is shown in Figure 13.

2.4.2 Control Circuit Voltage Regulation

The rectifier in the control circuit can output a DC voltage which varies from 0V to 48V. This raw DC signal can easily exceed the maximum input voltage of the sensors and microcontrollers. To mitigate this, a voltage regulation circuit was used. This circuit contains the LM2576HV regulation IC configured to limit the voltage from the rectifier to 12V.

To configure the LM2576HV regulator output to a peak output voltage of 12V, the following formula from the datasheet was utilized:

$$V_{\text{out}} = 1.23\left(1 + \frac{R_2}{R_1}\right),\ R_2 = 8.7\text{k}\Omega,\ R_1 = 1\text{k}\Omega \tag{2}$$

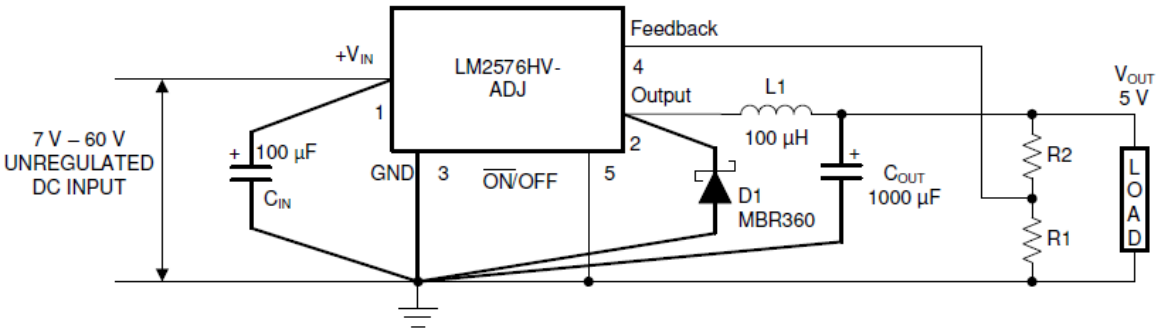

Figure 15: Diagram of General LM2576HV Regulator Circuit

This 12V signal from the regulator is then used to power the servo motor and control Arduino. The servo motor can then control the blade pitch which is crucial for controlling turbine operation and safety tasks. The control Arduino also has its own built in voltage regulators outputting 5V and 3.3V. The 5V regulated output from the Arduino Uno is used to power a wind speed sensor which uses a digital hot-wire technique as opposed to a traditional anemometer to obtain wind speed. The 3.3V regulated output from the Arduino is used to power the RPR220 IR Sensor. This IR sensor is embedded inside the generator assembly on top of one of the coil magnets. As the coil magnet rotates, a the RPR sensor will output a low value when it detects a dark surface (the magnet), and then output a high value when it detects a white dote painted on the magnet. The Arduino can then calculate the RPM of the turbine by identifying the number of high signals in a period of time.

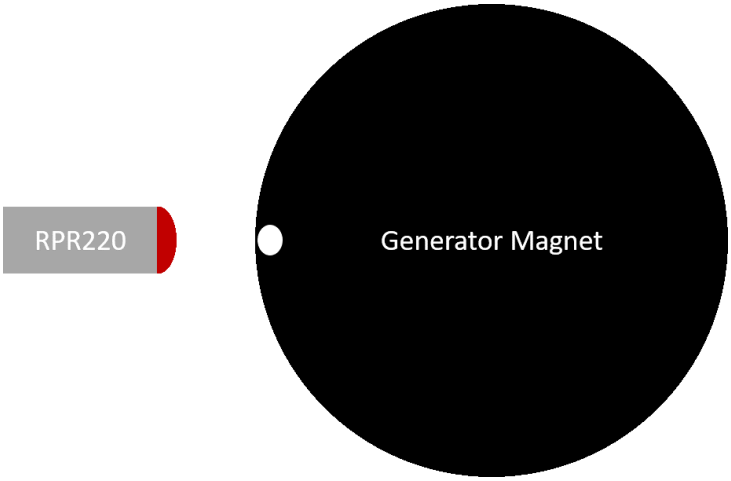

Figure 16: The RPR220 IR sensor is used to measure the generator RPM.

of the turbine by identifying the number of high signals in a period of time. The wind speed sensor works by heating up a resistor coil, and then calculates the wind speed by determining how much power is required to keep coil at a certain temperature. This process can draw a high level of current at high wind speeds. To account for this factor, the team chose to power the Arduino Uno with a 12V DC signal - which is the maximum input voltage it can handle - to make sure the Arduino has enough power to run at full capacity while also operating both the wind speed and RPM sensors.

2.4.3 Control Circuit Logic

During the turbine testing phase, a simplified version of the control circuit code was utilized. This code enabled quick changes of the blade pitch directly from the serial monitor of the control Arduino. An IR sensor was used to monitor generator RPM, and a wind speed sensor was included in the circuit design, but they both have not been fully integrated into the code of the control Arduino.

The primary control circuit code functions as the following: when the turbine is producing enough power to activate the control circuit computer, it will begin to pitch the turbine blades to the enable position.

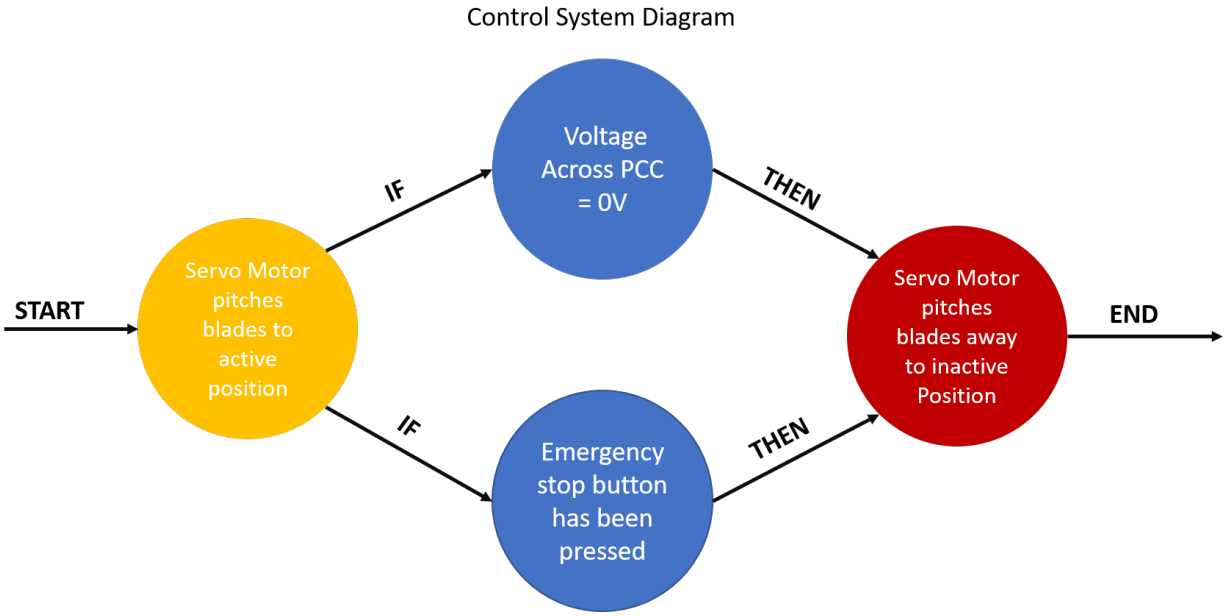

Figure 17: Visualization of the control circuit logic

This is the pitch that will produce maximum power. At this state, the computer will continuously loop to check the status of the voltage across the PCC, as well as monitor the status of the emergency stop button. If the voltage across the PCC is detected to be 0V or if the emergency stop bump switch has been activated, the servo motors will pitch the blades to the maximum forward position, so that the blades act as an air brake thus slowing the turbine to a stop.

2.4.4 Control Model Analysis

The functionality of the turbine will vary greatly depending on the environment it is placed in. There are four total functional states that are determined based on the physical wind speed of the environment. In region 1, the wind speed will be low ranging from 2.5 to 4.5 m/s. Region 2 is the “normal” operational state and it occurs when the wind speed ranges from 4.5 m/s to 11 m/s. Region 3 occurs at high wind speeds greater than 11 m/s. Finally, Region 4 is set when the turbine needs to immediately shut down.

2.4.5 Load Circuit

The load circuit consists of a current sensor, latching relay, LiPo battery, voltage buck/boost regulator, Arduino Pro Mini, and 50-ohm load resistor. The purpose of the current sensor is to detect when the load is disconnected. The latching relay is used to deliver power from the battery to the linear servos during the safety task. The LiPo battery and voltage buck/boost regulator are used together to power the load Arduino during all modes of operation and the linear servos when the load is disconnected or when the emergency stop button is depressed. The Arduino Pro Mini was chosen for its low power consumption and is used to toggle the latching relay and communicate with the current sensor. Lastly, the 50-ohm resistor is the main power dissipating element of the load. Due to limited lab access, the team was not able to determine the new optimal value for the resistor. As a result, the team elected to use the 50-ohm value, which was used in the 2019 competition.

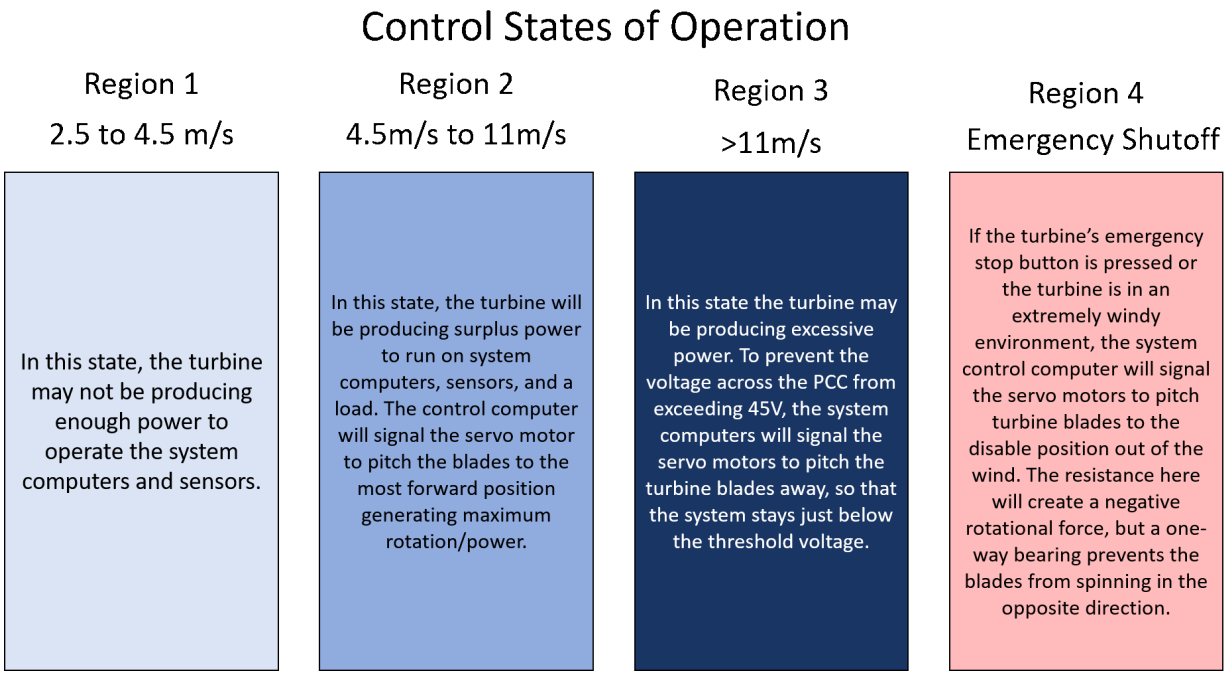

Figure 18: Description of control states for each of the turbine's three regions, plus emergency shutoff (Region 4).

3 Turbine Testing

For most of the year testing was unavailable due to the risks associated with the pandemic, fortunately, some initial testing was completed before the end of the year. The turbine underwent wind tunnel and dynamometer testing to gather data on the performance of the turbine. This data would both give insight on how the turbine as a whole can be optimized with the new two-bladed rotor, and ensure the generator is performing appropriately as compared to how it has performed in the past. The main issue faced in preparing the turbine was that one of the coil housings had a broken foot, which prevented it from sitting in the stator in a secure fashion. This issue was remedied by preparing a new housing and replacing the broken one.

3.1 Testing Objective

Since lab access was limited, the main objective for testing was to understand how the turbine performs with a two-bladed rotor and within the parameters of the competition. Wind tunnel testing was done to better understand how the new rotor performs under various conditions. Dynamometer testing was done to see how the generator performs compared to last year as well as to see how the generator performs at the extremes of the competition. One final objective it to ensure the turbine produces enough voltage at cut-in velocity to power an Arduino, which will be used to control the pitch of the blades.

3.2 Testing Procedure

Wind tunnel testing was done qualitatively, with the exception of completing the Arduino objective, so data points were not extensively collected. The two-bladed rotor was fitted with the nylon-12 blades and the output current, voltage, and power were monitored during testing on an electric load. The RPM was

kept within the predicted parameters of optimal performance and measured using a strobe light.

The cut-in velocity was determined to be 2.5 m/s, which is an improvement from the three-blade rotor design. At this velocity the turbine produced 5V, which is enough to power an Arduino. To determine how the behavior of the rotor speed, the wind velocity was increased to a maximum of 9 m/s (uncorrected) and the turbine did not exceed the predicted threshold for optimal tip speed ratio (TSR) of 1900 RPM.

Since dynamometer testing was more readily accessible, additional general and specific testing was done. General testing showed that the generator was performing comparably to previous years, therefore no immediate repairs had to be made after replacing a coil housing. The next round of testing was strength testing. In this round of testing, we tested the limits of the generator within the parameters of the competition. Our results indicated that the limits of the turbine system are mainly controlled by the maximum current allowable through the stators, which indicates that the voltage limit of the competition will be satisfied if the current is monitored.

3.3 Testing Results

Figure 19 is the culmination of the dynamometer testing. It shows the power curves produced by the dynamometer at various load resistances. The results show that the generator is still performing as well as in previous years . If more time was available for testing, wind tunnel data would be provided showing power output in comparison to the predicted power output. This data would be crucial to deter mining the turbine's operating range and finding the optimal electronic load resistance, which could be programmed into the control Arduino to optimize power production.

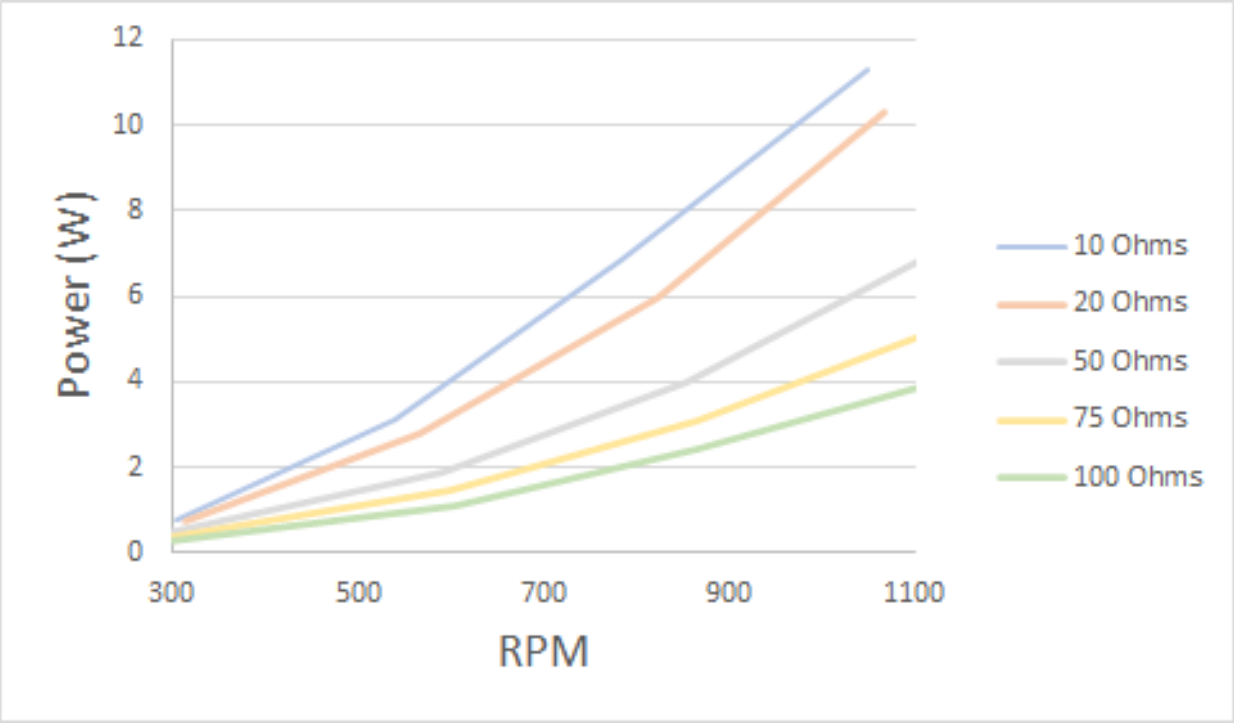

Figure 19: Generator code predicted power (red) overlaid with results from dynamometer testing.

4 Commissioning Checklist

For wind tunnel testing, the following commissioning checklist can be used to ensure that the turbine is fully operational. The critical parts to check are that the rotor is correctly secured and that the control circuit can be used to change the rotor pitch to prevent the rotor from spinning uncontrollably in the high wind speed test.

PSU Wind Energy Club
Commissioning Checklist for Wind Tunnel Testing

Activity (once the turbine is installed, double-check each of these)	Completed?	
Attach the test stand to the nacelle		
Assemble the generator in the nacelle		
Position the rotors and stators so the stators line up with the holders on the nacelle cover		
Thread the rotor shaft through the nacelle, rotors, and stators and secure with a one-way clutch bearing and two-way bearings		
Use the aluminum foil slips to space the rotors and stators appropriately before screwing in		
Attach servos to nacelle		
Connect wires to generator stages and servos and run through the test stand pipe		
Assemble the rotor, attaching the hub and pithing mechanism before the blades		
Thread the rotor onto the shaft and position the hub so that the pitching mechanism has an effective range of motion		
Assemble the servo-pitching subsystem		
Attach the collar to the pitching mechanism		
Attach the subsystem arms to the collar using the pins		
Attach the arms to each linear servo		
Attach the tailfin to the rear of the nacelle		
Secure the nacelle cover onto the top of the nacelle		
Assemble the circuits and controls box		
Put the turbine in the wind tunnel, threading the wires through the hole in the floor. Bolt the turbine down		
Connect the wires to the load and controls circuit for the generator stages and servo		
Calibrate the linear servos for control		

5 Building on Previous Years' Work

The Penn State Wind Energy Club has a strong history in the Collegiate Wind Competition, particularly with regards to the physical turbine. The team has continued to use components developed in previous years. Notably, the team's in-house generator continues to be used since it has a very low startup torque compared to off-the-shelf generators available. In the 2022 year, the team aims to reconsider the generator design and further optimize the axial flux design. Additionally, the team is using the same nacelle as in

previous years since it is already designed with the current generator in mind. The nacelle also allows for the same rotor shafts to be used as previously, which are compatible with the new hub for the two-bladed rotor. The team has also continued to use the same tailfin as in previous years since its dimensions still fit within the box, and it attaches easily to the nacelle. Within the circuits and controls subsystem, the framework of the control and load circuit is much like that of the 2019 competition year. This is because a redesign would not be feasible due to issues obtaining lab access during the pandemic. Despite this, some improvements have been made to design, specifically in the control circuit. A wind speed sensor and RPM sensor were implemented to provide data to optimize pitch angle for maximum turbine performance. In the past, optimal pitch angle values were determined through extensive experimental testing. Specifically, the turbine computers would estimate wind speed from the voltage being produced by the Turbine, but this system only works well in one specific geographic location where air density is constant. By directly obtaining the generator RPM, and wind speed, a more accurate method of optimized pitch control can be obtained. The team also modified the voltage regulation circuit within the control circuit to improve circuit stability.

6 Conclusions

The Penn State Wind Energy Club's 2021 competition turbine is an improvement upon previous years' turbine systems. Most notably, the rotor has changed from three blades to two blades, which has two primary advantages. It increases the Reynolds number experienced by the blades which results in higher airfoil glide ratios and increased power production. It also reduces the effects of stall, making the rotor more consistent in startup at low tip speed ratios where the pitch is fixed because the turbine is not producing enough power to control the Arduino. Another important design change is the replacement of the radial servo with a pair of linear servos, which allows for more precise and accurate control of the blade collective pitch for turbine control. The control circuit has also been simplified and documented for use in future years. The team has been able to improve upon the club's existing turbine despite the numerous challenges presented by the past year's remote working conditions. Testing and experimentation was extremely limited due to restrictions on lab availability, especially not gaining access to any lab space until mid March. The majority of the work was completed across video calls, slack, and shared documents.

References

[1] Align 700. http://www.align.com.tw/helicopter-en/trex700/. Accessed: 05-23-2021.

[2] Mark Drela. XFOIL: An analysis and design system for low Reynolds number airfoils. Low Reynolds number aerodynamics lecture notes, 1989.

[3] Sven Schmitz. XTURB-PSU, 2017.

[4] Sven Schmitz. *Aerodynamics of Wind Turbines: A Physical Basis for Analysis and Design*. John Wiley & Sons, 2020.

[5] Michael S Selig. *Summary of low speed airfoil data*. SOARTECH publications, 1995.